GU J Sci, Part C, 11(1): 210-221 (2023)

Gazi University

Journal of Science

PART C: DESIGN AND TECHNOLOGY

http://dergipark.gov.tr/gujsc

Investigation of the Thermal Properties of Cu-based Shape Memory Alloy

Neslihan TURAN,

Gazi University, Faculty of Science, Department of Physics, 06500, Yenimahalle/Ankara/TÜRKİYE

Article Info

Research article
Received:28/10/2021
Revision:14/04/2021
Accepted:26/11/2022

Keywords

Thermal properties
Shape memory alloy
Activation energy
Martensitic transition

Abstract

This study aims to investigate the thermal properties of the phase transformation that may occur with the effect of temperature in Cu-14.70wt.%Al-4.72wt.%Ni shape memory alloy. The sample was annealed at 1203 K for 30 min in an argon atmosphere and then cooled rapidly in salt-ice water. By using Differential Scanning Calorimetry (DSC), the martensitic phase transformation parameters of the sample were found. The activation energy required for these transformations was calculated using the Kissinger, Augis-Bennett, and Takhor methods. Thermogravimetric Analysis (TGA) measurements investigated the mass changes that may occur with the effect of temperature. Surface morphology was analyzed using an optical micrograph.

1. INTRODUCTION

Factors such as pressure, hardness, and temperature cause microstructural changes in some metals and alloys. Because of these effects, transformations in which the neighborhood of atoms does not change, but the crystal structure changes are called "martensitic phase transformations" [1]. In these transformations, the high-temperature phase is defined as “austenite” and the low- temperature phase is defined as “martensite” While the austenite crystal structure is in thermodynamic equilibrium at T_0, if the material is cooled, a martensite structure begins to form within the austenite structure at a critical temperature value (M_s). The transformation that starts at M_s temperature occurs in a certain temperature range and the temperature at which the transformation ends is called the “martensite finish temperature (M_f). The martensitic transformation is reversible, as the martensite sample returns to the austenite structure, which is the main phase when heated. In this way, having different configurations above and below a critical transformation temperature is defined as "shape memory” [2]. Shape memory alloys (SMA) are materials used in many applications including biomedical, automotive, and aerospace fields [3–5]. The most known and most studied SMAs are titanium and nickel alloys. Although nitinol (Ni-Ti), which is characterized by the high stability of the martensitic phase, has several positive properties such as mechanical strength and corrosion resistance, special production techniques are required due to the high cost of the material and the high reactivity of titanium. Therefore, Cu-based SMAs have attracted attention not only as a low-cost alternative to the mechanical applications of nitinol but also for other applications with their superior electrical and thermal conductivity and the possibility of increasing resistance [6, 7]. In Cu-based alloys, the shape memory effect is strongly dependent on thermal treatments, mechanical effects, and element ratios in the structure and production methods [8–13]. Another property of Cu-based SMAs is superelasticity, which allows for high elastic deformations of up to 14%, making them suitable for storage and dissipation of mechanical energy [1, 14, 15].

In this study, the phase transformation properties of Cu-14.70wt.% Al-4.72wt.% Ni alloy were investigated because the transformation temperature values are close to ambient conditions and it has thermal stability at high temperatures [16]. Differential scanning calorimetry (DSC) measurements were carried out from

Corresponding author, e-mail: neslihanturan@gazi.edu.tr DOI: 10.29109/gujsc.1196035

room temperature to 423 K at 10K/min, 15K/min, 20K/min, 25K/min, and 30K/min heating The activation energy required for the transformations was evaluated using the Kissinger, Augis-Bennett, and Takhor methods. By using thermogravimetric analysis (TG), mass changes that may occur with the effect of temperature, and surface morphology were examined using an optical micrograph.

2. MATERIALS AND METHODS

The Cu-14.70wt.%Al-4.72wt.%Ni shape memory alloy studied in this study was purchased from Trefimetaux Center de Recherche in France. Samples were obtained from the alloy in the form of a rod with a length of 250 mm and a diameter of 4 mm, to be used in experimental processes. A special quartz tube was used to minimize the oxidation during the annealing and cooling process. Ar gas was released from a valve of the tube and vacuumed from the other valve by a mechanical pump. This process was repeated 8–10 times to avoid air in the tube. The samples were annealed for 30 min at 1203 K in Ar atmosphere in a special quartz be in to eliminate the effect of cutting and to ensure homogenization. After heat treatment, the samples were cooled rapidly by immersing the quartz tube in salt-ice water. DSC measurements were performed to determine the transformation characteristic such as transformation temperatures, enthalpy (ΔH) and entropy change values (ΔS) of transformation, and activation energy. Measurements were carried out from room temperature to 423 K at 10K/min, 15K/min, 20K/min, 25K/min, and 30K/min heating rates with a 14.8 mg sample using a Perkin Elmer Sapphire model DSC. The 28.004 mg powder sample was heated in an argon gas atmosphere and the change in mass due to the effect of temperature was investigated using a Perkin Elmer Pyris Diamond thermal analyzer.

The changes in the properties of the material, such as mass, enthalpy, and entropy depending on temperature, are analyzed using thermal analysis techniques. These techniques have various uses in thermally changing materials such as glass, ceramics, superconductors, metals, semiconductors, pharmaceuticals, and polymers. In the DSC method, while the same temperature is applied to the reference material and the sample, in case the sample temperature changes, the reference material or sample is maintained at the same temperature by giving external heat. According to the working principle of DSC, the energy change in the sample is compared the energy change of the reference material, and the difference between the energies is observed as peaks in the measurement results. That is, the DSC curves are the graphs of the energy change depending on the temperature. Because of the exothermic or endothermic reaction in the sample, peaks are seen in the DSC curves. The activation energy can be calculated because of the shift of the peaks depending on the heating rates. Fig. 1 shows how to find austenite start (A_s), austenite finish (A_f), martensite start (M_s), and martensite finish (M_f) temperatures from DSC curves [17].

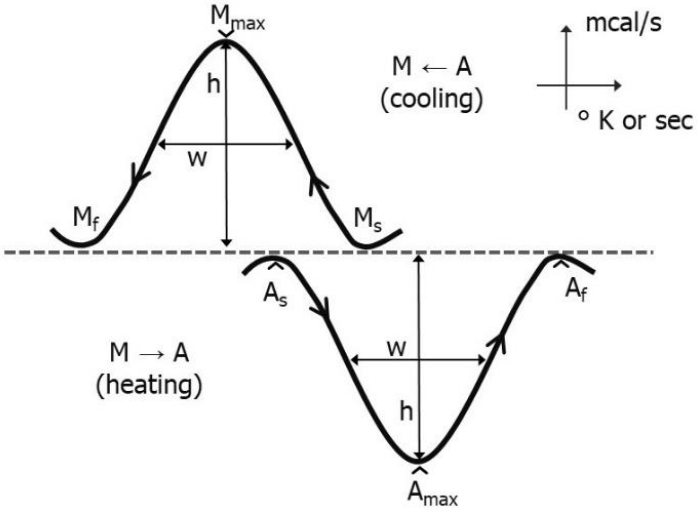

Figure 1. *Schematic DSC curve of M→A and A→M transformation (M_s, M_{max}, M_f, A_s, A_{max}, A_f; transformation temperatures and h; the peak height and w peak width at 1/2 –height) [17]*

In the austenite–martensite phase transformation, the volume changes with the change in the crystal structure. When the volume of an isolated system changes from V_1 to V_2 while the pressure (P) is constant; according to the first law of thermodynamics, energy changes from E_1 to E_2, and (ΔE) is;

$$\Delta E = E_2 - E_1 = \Delta Q - P(V_2 - V_1) \tag{1}$$

From Eq.1, we find that the change in heat of the system (ΔQ);

$$\Delta Q = (E_2 + PV_2) - (E_1 + PV_1) \tag{2}$$

"the total heat content of a system" or "enthalpy (H)" is given in Eq. 3. In that case; ΔQ

$$H = E + PV \tag{3}$$

$$\Delta Q = H_2 - H_1 \tag{4}$$

If the specific heat difference of the austenite and martensite phases is neglected, the entropy change of the sample (ΔS) will be the same for both transformations, although the heat measured in the austenite-martensite transformation is higher in absolute value than the temperature measured in the martensite-austenite transformation [18]. In phase transformations such as evaporation and melting, the temperature of the system does not change despite the energy change, provided that P remains constant. Therefore, ΔS must be calculated at a constant temperature. Accordingly, the derivative of H at a constant P;

$$\Delta H = \Delta E + P\Delta V \tag{5}$$

From the first law of thermodynamics, we find that

$$\Delta E = \Delta Q - P\Delta V \tag{6}$$

$$\Delta H = \Delta Q \tag{7}$$

At constant P; ΔS is given by Eq. 8 and evaluated using Eq. 9 [19].

$$\Delta S = \frac{\Delta Q}{T} = \frac{\Delta H}{T} \tag{8}$$

$$\Delta S_{M\rightarrow A} = \Delta H_{M\rightarrow A} / T_0 \tag{9}$$

According to Salzbrenner and Cohen [20] and Tong and Wayman [21], T_0 is the equilibrium temperature and is determined by Eq. 10 and Eq. 11, respectively.

$$T_o = \frac{1}{2}(M_s + A_s) \tag{10}$$

$$T_o = \frac{1}{2}(M_s + A_f) \tag{11}$$

Activation energy

The activation energy of phase transition can be calculated using shifts in exothermic peak temperature values with different heating rates. The Kissinger, Takhor, and Augis-Bennett methods were used to

calculate the activation energy (E_a) [22, 23]. According to the Kissinger method, the Activation energy is calculated using Eq. 12.

$$\frac{dln(\frac{\beta}{T_x^2})}{d(\frac{1}{T_x})} = -\frac{E_a}{R} \tag{12}$$

where β is the heating rate, T_x is the peak value of the endothermic or exothermic reaction, (A_{max} or M_{max}), and R is the gas constant (R=8.314 j/molK). The activation energy was evaluated from the slope of the ln (β/T_x^2)-1000/T_x plot.

According to the Takhor method, the activation energy is calculated using Eq. 13. The slope of the lnβ-(1000/T_x) plot is replaced in Eq. 13.

$$\frac{dln(\beta)}{d(\frac{1}{T_x})} = -\frac{E_a}{R} \tag{13}$$

According to the Augis-Bennett method, the activation energy is calculated using the slope of the ln ($\beta/(T_x-T_m)$)-(1000/T_x) graph with Eq. 14 [23]. Where T_m is the absolute temperature.

$$\frac{dln(\frac{\beta}{T_x-T_m})}{d(\frac{1}{T_x})} = -\frac{E_a}{R} \tag{14}$$

In the thermogravimetric analysis method, the change in the mass of the sample with an increase in temperature is analyzed. In temperature-mass change curve, called a thermogram, there may be a mass increase in the sample due to oxidation with the effect of temperature, as well as mass loss due to the decomposition of impurities or evaporation of components such as water. In this study, the change in the mass of the 28.004 mg powder sample with the effect of temperature was investigated in the argon gas atmosphere. Measurements were performed using a Perkin Elmer Pyris Diamond thermal analyzer. Surface morphology was characterized by optical micrographs.

3. RESULTS

DSC curves obtained from the 14.8 mg sample with a heating rates of 10K/min, 15K/min, 20K/min, 25K/min, and 30K/min are shown in Fig. 2. In these curves, the direction of the endothermic reaction is downward. In the DSC curves, it is seen that while the temperature rises from 290 K to 425 K, the sample shows an endothermic reaction, that is, it takes energy from the system. While the sample is cooling, it is seen that it shows an exothermic reaction, that is, energy is given to the system from the sample, with peaks formed in the up and down directions.

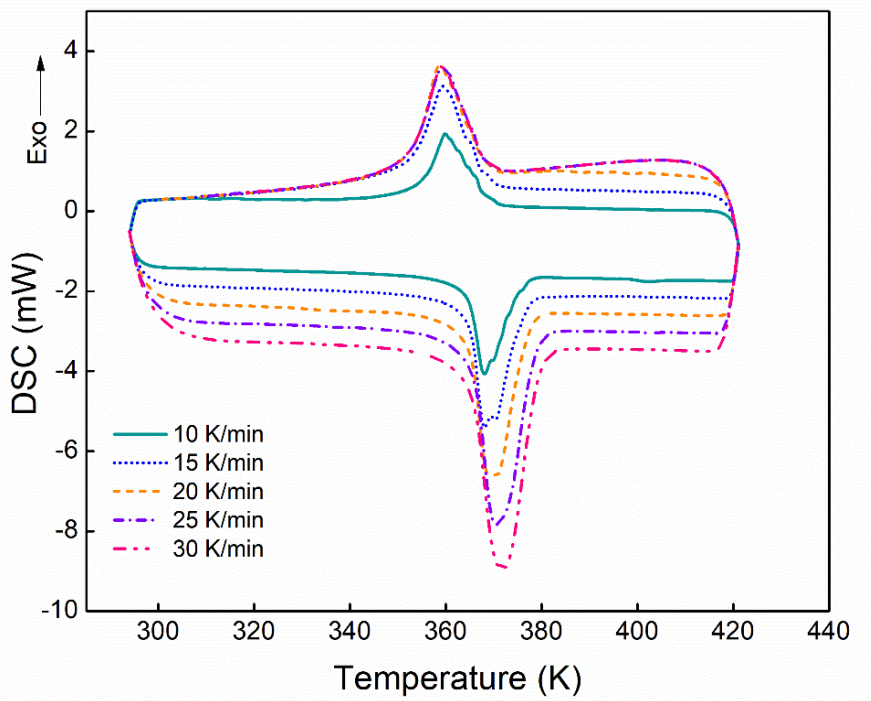

Figure. 2. *DSC curves of the sample at 10 K/min, 15 K/min, 20 K/min, 25 K/min, and 30 K/min heating rates*

During heating, a transition occurs from the martensite to the austenite phase and during cooling, a transition from the austenite phase to martensite occurs. When Fig. 2, which shows the DSC curves taken according to different heating rates, is examined, it is seen that there is an increase in the peak intensities of both reactions directly proportional to the heating rates, and a shift in the transformation temperatures. The shape of the peak is related to the heating rate, thermal conductivity, heat capacity and shape of the sample, and the amount of heat transferred [24]. The increase in peak intensity depends on the heat flow rate. The kinetic parameters obtained from the DSC curves at different heating rates and the T_0 values calculated using Eq.10 and Eq.11 are shown in Table 1. The martensite-austenite phase transformation during heating started at 364.59 K and was completed at 379.31 K, according to the heating rates. As the heating rate increased, the A_s and A_f temperatures increased. During cooling, the austenite-martensite transformation started at 368.33 K and was completed at 352.59 K, depending on the heating rate.

Table 1. The kinetic parameters obtained from the DSC curves at different heating rates and the T_0 values calculated using Eq.10 and Eq.11

Heating rate	A_s (K)	A_{max} (K)	A_f (K)	M_s (K)	M_{max} (K)	M_f (K)	$T_0(1)$ (K)	$T_0(2)$ (K)
10K/min	364.59	368.1	374.38	368.12	359.86	354.43	366.355	371.25
15K/min	364.85	368.1	375.82	368.3	359.34	352.68	366.575	372.06
20K/min	364.88	370.64	376.72	367.26	358.85	352.94	366.07	371.99
25K/min	365.45	370.57	378.36	368.14	359.29	352.59	366.795	373.25
30K/min	365.10	371.74	379.31	368.33	359.1	352.76	366.715	373.82

The enthalpy change values obtained from DSC measurements using Eq. 8 and the entropy change values calculated using Eq.9 are given in Table 2. $\Delta H_{M\rightarrow A}$ and $\Delta S_{M\rightarrow A}$ represent martensite-austenite, and $\Delta H_{A\rightarrow M}$

and $\Delta S_{A\rightarrow M}$ represent enthalpy and entropy changes of austenite-martensite transformation, respectively. $\Delta S_{M\rightarrow A}(1)$ and $\Delta S_{A\rightarrow M}(1)$ were calculated using Eq.10, and $\Delta S_{M\rightarrow A}(2)$, and $\Delta S_{A\rightarrow M}(2)$ were calculated using Eq.11.

Table 2. Variation in enthalpy and entropy values for phase transformations

Heating rate	$\Delta H_{M\rightarrow A}$ (10^3J/kg)	$\Delta H_{A\rightarrow M}$ (10^3J/kg)	$\Delta S_{M\rightarrow A}(1)$ (J/kg K)	$\Delta S_{M\rightarrow A}(2)$ (J/kg K)	$\Delta S_{A\rightarrow M}(1)$ (J/kg K)	$\Delta S_{A\rightarrow M}(2)$ (J/kg K)
10K/min	-7.94	7.45	-21.68	-21.39	20.34	20.07
15K/min	-8.20	9.46	-22.37	-22.04	25.81	25.43
20K/min	-8.17	8.37	-22.32	-21.97	22.87	22.50
25K/min	-8.08	6.80	-22.03	-21.65	18.54	18.22
30K/min	-8.07	5.98	-22.01	-21.59	16.31	16.00

When Table 2 is examined, it is seen that the enthalpy and entropy change values change depending on the heating rate. In the martensite-austenite transformation, the enthalpy is in the range of $7.94x10^3$ J/kg-$8.20x10^3$ J/kg, and in the austenite-martensite transformation, it is in the range of $5.98x10^3$ J/kg-$9.46x10^3$ J/kg. Entropy change values are in the range of 21.39 J/kgK and 22.37 J/kgK in martensite-austenite transformation, and 16.31 J/kgK-25.81 J/kgK in austenite-martensite transformation. Enthalpy and entropy change values in martensite-austenite transformation are lower than enthalpy and entropy change values in recycling. The enthalpy value can give us an idea of whether the transformation is partial or full [9]. Since the expected enthalpy value for the full transformation to occur is $10x10^3$ J/kg, it is seen that the martensitic transformation rate is very high in measurements at a heating rate of 15 K/min.

The activation energy value of the sample according to the Kissinger method was calculated as 272.53 kJ/mol using Eq. 12 from the ln (β/T_x^2)-$1000/T_x$ plot given in Fig. 3.

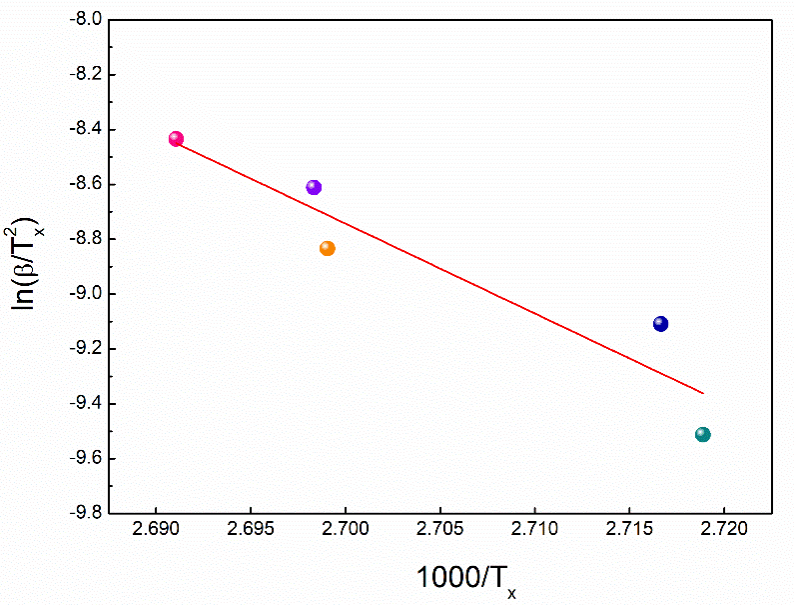

Figure 3. *ln (β/T_x^2) - $1000/T_x$ plot obtained from DSC curves for the Kissinger method*

The activation energy value of the sample according to the Takhor method was calculated as 278.67 kJ/mol using Eq. 13 from the ln (β)-1000/T_x plot given in Fig. 4

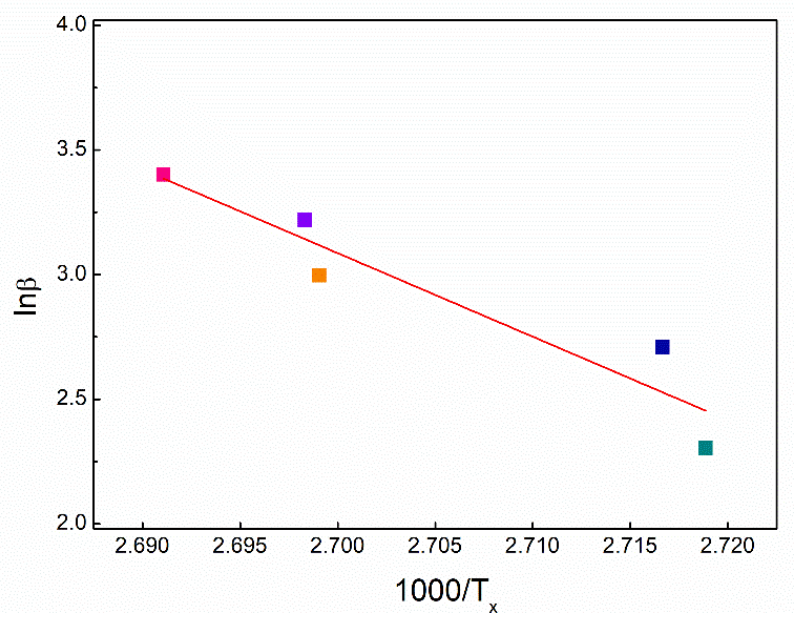

Figure 4. *ln (β)-1000/T_x plot obtained from DSC curves for the Takhor method*

The activation energy value of the sample according to the Augis-Bennett method was calculated as 262.30 kJ/mol using Eq. 14 from the ln ($\beta/(T_x-T_m)$)-($1000/T_x$) plot given in Fig. 5

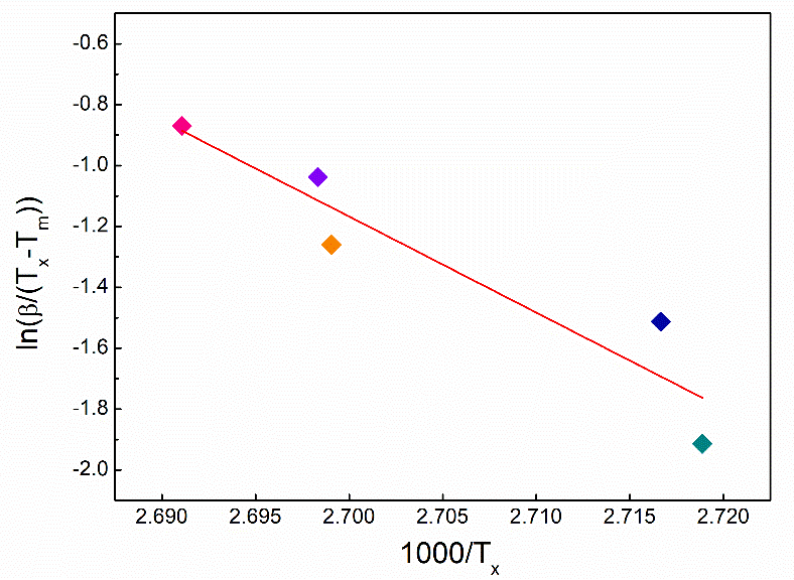

Figure 5. *ln ($\beta/(T_x-T_m)$)-($1000/T_x$) plot obtained from DSC curves for the Augis-Bennett method*

Approximate results were obtained in the activation energy values calculated using three different theoretical methods.

TGA measurements were performed to examine the changes that may occur in the mass of the sample with the effect of temperature. Fig. 6 shows the change in the mass of the 28.004 mg powder sample when heated in an argon gas atmosphere from room temperature to 1203 K, at a heating rate of 20 K/min.

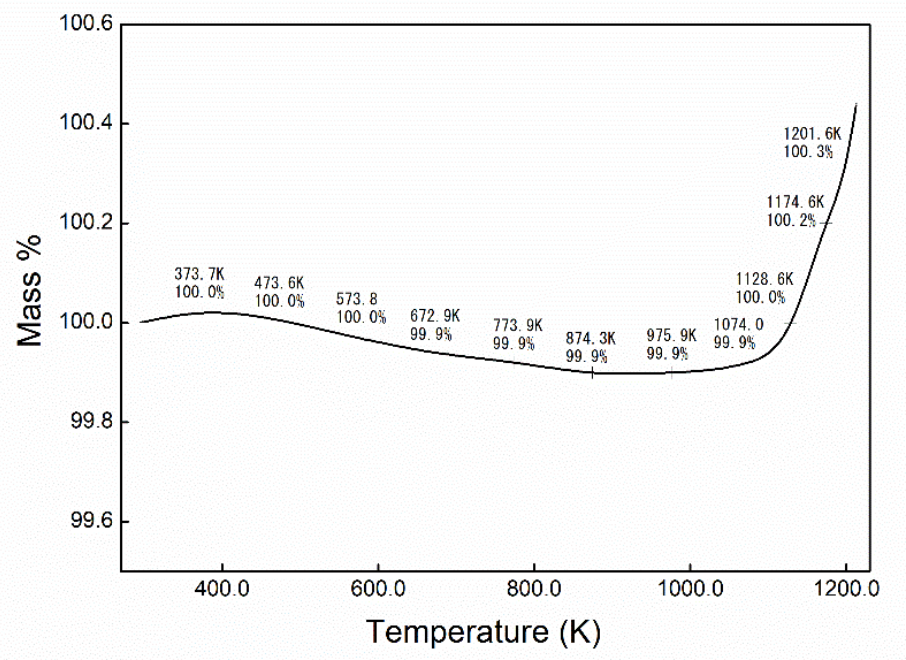

Figure 6. *TGA curve at 20K/min heating rate*

When Fig. 6 is examined, it is seen that there is no change in the sample mass up to 573.8 K, but there is a 0.1% loss between 573.8 K and 672.9 K. This loss in mass means that volatile components in the material evaporate or impurity decompose. material mass; It remained constant between 672.9 K and 1074.0 K and increased in direct proportion to the temperature after 1074.0 K. This increase indicates that the sample starts to oxidize after 1074.0 K. Between 1074.0 K and 1201.6 K, the total mass increase was 0.4%.

After heat treatment, the surface morphology of the sample was examined using an optical microscope with a Prior Panasonic digital camera. The sample with a thickness of 3–4 mm was fixed in bakelite for ease of sanding and polishing as seen in Fig. 7.

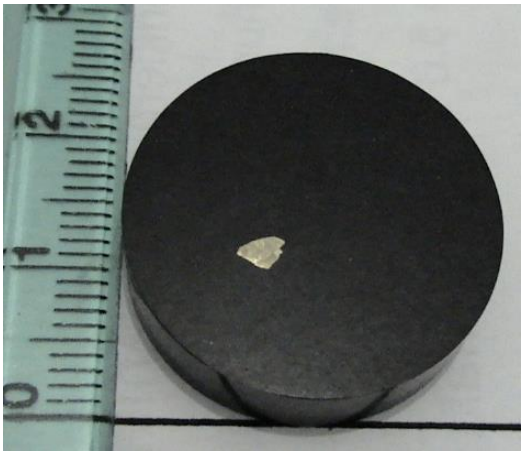

Figure 7. *An image of the sample*

The sanded and polished sample was washed with alcohol and etched with ($FeCl_3$-$6H_2O$)+ (CH_6OH)+(HCl) solution to remove dirt, oil, and rust on the surface. Images obtained with different magnifications from the sample surface are shown in Fig. 8.

(a)

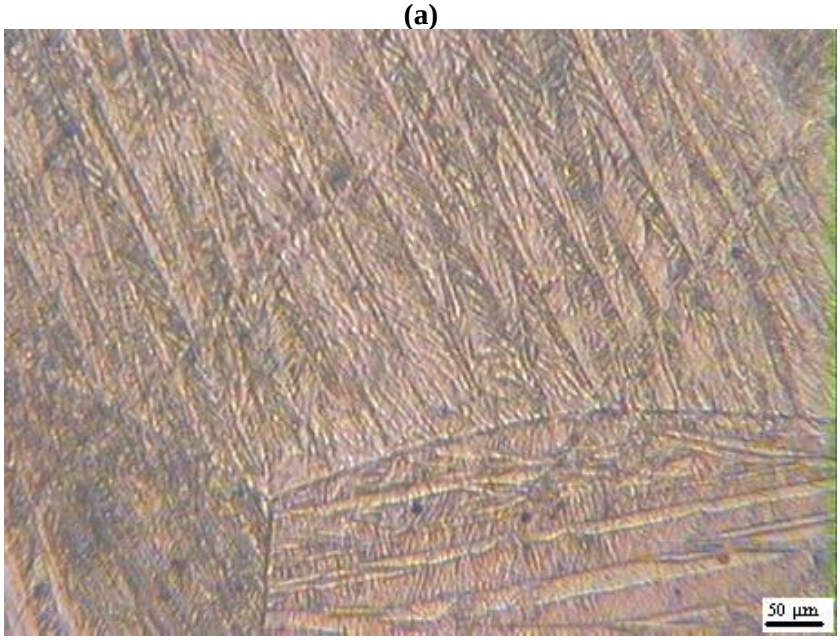

(b)

Figure 8. *Optical micrograph of the sample at different magnifications a) x100 b) x400*

Fig. 8a shows the surface pictures of the alloy taken at room temperature at x100 magnification and Fig. 8b at x400 magnification. The sample is in the martensite phase at room temperature. In the figures, it is observed that the grain boundaries were clear. The martensitic structure is densely dispersed in the grains. It is seen that these are V-type in some regions and needle-type in some regions.

4. CONCLUSIONS

The properties of Cu-based shape memory alloys are strongly dependent on thermal treatments, mechanical effects, and element ratios in the structure. In this study, the martensitic transformation parameters of Cu-14.70wt.%Al-4.72wt.%Ni alloy, which have not been studied before, were determined. In the martensitic phase transformation of Cu-14.70wt.%Al-4.72wt.%Ni shape memory alloy; transformation temperatures, activation energy, enthalpy, and entropy values were investigated using DSC, and mass changes depending on temperature were investigated using TGA. Using the optical micrograph surface morphology was analyzed.

When the DSC measurement results were examined, it was seen that the sample had the martensite phase at room temperature. While the martensite-austenite phase transformation occurred with an endothermic reaction between 364.59 and 379.31 K, the austenite-martensite phase transformation occurred with an exothermic reaction between 368.33 K and 352.68 K. The phase transformation temperature varies depending on the heating rate. Using the DSC measurements performed at the different heating rates, the activation energy was found 272.53 kJ/mol by the Kissinger method, 262.30 kJ/mol by the Augis-Bennett method, and 278.67 kJ/mol by the Takhor method. The results obtained using the three different methods are compatible with each other. The transformation parameters of this alloy show a dependence on temperature. According to the calculated enthalpy values, it was found that the highest conversion rate was obtained at a heating rate of 15 K/min, and it had a high transformation rate.

With the TGA measurement, the changes that may occur in the alloy mass in the annealing process were determined. The sample mass, which did not change up to 373.7 K, suffered a loss of 0.1% between 573.8 K and 672.9 K with the decomposition of impurities in the material. Then, the amount of mass did not change between 672.9 K and 1074.0 K but increased proportionally to the temperature after 1074.0 K. The total mass increase between 1074.0 K and 1201.6 K was calculated as 0.4%.

When the optical micrograph of the Cu-14.70wt.%Al-4.72wt.%Ni was examined, it was observed that the grains were polygonal, the grain boundaries were clear, and the grains were generally large, but there were a few small grains. The martensite phase structure, which can be observed at room temperature and is densely dispersed in the grains, appeared as a “V” in some regions and as a needle in some regions. Metallographic observations were consistent with the literature. [25, 26]

ACKNOWLEDGEMENTS

I would like to thank my thesis advisor, Prof. Dr. İrfan AKGÜN, who guided me with his valuable contributions throughout my studies and whose name I could not write to this study due to his death (2006).

I would like to thank Prof. Dr. Şükrü ÇAVDAR, Prof. Dr. Haluk KORALAY, and Prof. Dr. Yıldırım AYDOĞDU for their contributions to my thesis.

REFERENCES

1. Nishiyama Z, Fine ME, Meshii M, Wayman CM (1978) Martensitic transformation. Academic Press, London

2. Perkins J (1975) Shape Memory Effects in Alloys. Springer Science+Business Media, LLC, California

3. Van Humbeeck J (2001) Shape memory alloys: A material and a technology. Adv Eng Mater 3:837–850. https://doi.org/10.1002/1527-2648(200111)3:11<837::AID-ADEM837>3.0.CO;2-0

4. Mohd Jani J, Leary M, Subic A, Gibson MA (2014) A review of shape memory alloy research, applications and opportunities. Mater Des 56:1078–1113. https://doi.org/10.1016/j.matdes.2013.11.084

5. Chen Q, Thouas GA (2015) Metallic implant biomaterials. Mater Sci Eng R Reports 87:1–57. https://doi.org/10.1016/j.mser.2014.10.001

6. Gojić M, Vrsalović L, Kožuh S, et al (2011) Electrochemical and microstructural study of Cu-Al-Ni shape memory alloy. J Alloys Compd 509:9782–9790. https://doi.org/10.1016/j.jallcom.2011.07.107

7. Alaneme KK, Anaele JU, Okotete EA (2021) Martensite aging phenomena in Cu-based alloys: Effects on structural transformation, mechanical and shape memory properties: A critical review.

Sci African 12:. https://doi.org/10.1016/j.sciaf.2021.e00760

8. Canbay CA, Karagoz Z (2013) Effects of Annealing Temperature on Thermomechanical Properties of Cu-Al-Ni Shape Memory Alloys. Int J Thermophys 34:1325–1335. https://doi.org/10.1007/s10765-013-1486-z

9. Niedbalski S, Durán A, Walczak M, Ramos-Grez JA (2019) Laser-assisted synthesis of Cu-Al-Ni shape memory alloys: Effect of nert gas pressure and Ni content. Materials (Basel) 12:. https://doi.org/10.3390/MA12050794

10. Ozbulut OE, Hurlebaus S, Desroches R (2011) Seismic response control using shape memory alloys: A review. J Intell Mater Syst Struct 22:1531–1549. https://doi.org/10.1177/1045389X11411220

11. Pereira EC, Matlakhova LA, Matlakhov AN, et al (2016) Reversible martensite transformations in thermal cycled polycrystalline Cu-13.7%Al-4.0%Ni alloy. J Alloys Compd 688:436–446. https://doi.org/10.1016/j.jallcom.2016.07.210

12. Payandeh Y, Mirzakhani B, Bakhtiari Z, Hautcoeur A (2022) Precipitation and martensitic transformation in polycrystalline CuAlNi shape memory alloy – Effect of short heat treatment. J Alloys Compd 891:162046. https://doi.org/10.1016/j.jallcom.2021.162046

13. Pushin VG, Kuranova NN, Svirid AE, et al (2022) Design and Development of High-Strength and Ductile Ternary and Multicomponent Eutectoid Cu-Based Shape Memory Alloys: Problems and Perspectives. Metals (Basel). 12:1289

14. Lattanzi MG, Sozzetti A (2010) Gaia and the Astrometry of Giant Planets. Cambridge University Press, Cambridge

15. Chen Y, Schuh CA (2011) Size effects in shape memory alloy microwires. Acta Mater 59:537–553. https://doi.org/10.1016/j.actamat.2010.09.057

16. Miyazaki S, Otsuka K (1989) Development of Shape Memory Alloys. ISIJ Int 29:353–377. https://doi.org/10.2355/isijinternational.29.353

17. Perkins J, Muesing WE (1983) MARTENSITIC TRANSFORMATION CYCLING EFFECTS IN Cu-Zn-Al SHAPE MEMORY ALLOYS. Metall Trans A, Phys Metall Mater Sci 14 A:33–36. https://doi.org/10.1007/BF02643734

18. Ortín J, Planes A (1988) Thermodynamic analysis of thermal measurements in thermoelastic martensitic transformations. Acta Metall 36:1873–1889. https://doi.org/10.1016/0001-6160(88)90291-X

19. Xu H, Tan S (1995) Calorimetric investigation of a Cu-Zn-Al alloy with two way shape memory. Scr Metall Mater 33:749–754. https://doi.org/10.1016/0956-716X(95)00269-2

20. Salzbrenner RJ, Cohen M (1979) On the thermodynamics of thermoelastic martensitic transformations. Acta Metall 27:739–748. https://doi.org/10.1016/0001-6160(79)90107-X

21. Tong HC, Wayman CM (1975) Thermodynamics of thermoelastic martensitiC transformations. Acta Metall 23:209–215. https://doi.org/10.1016/0001-6160(75)90185-6

22. Lawner BJ, Mattu A (2012) Cardiac Arrest. In: Cardiovascular Problems in Emergency Medicine: A Discussion-based Review. pp 123–137

23. Augis JA, Bennett JE (1978) Calculation of the Avrami parameters for heterogeneous solid state reactions using a modification of the Kissinger method. J Therm Anal 13:283–292. https://doi.org/10.1007/BF01912301

24. Höhne GWH, Hemminger WF, Flammersheim H-J (2003) Differential Scanning Calorimetry, 2nd ed. Springer Berlin, Heidelberg, Berlin, Heidelberg

25. Aydogdu Y, Aydogdu A, Adiguzel O (2002) Self-accommodating martensite plate variants in shape memory CuAlNi alloys. J Mater Process Technol 123:498–500. https://doi.org/10.1016/S0924-0136(02)00140-1

26. Recarte V, Pérez-Landazábal JI, Ibarra A, et al (2004) High temperature β phase decomposition processin a Cu-Al-Ni shape memory alloy. Mater Sci Eng A 378:238–242. https://doi.org/10.1016/j.msea.2003.09.111